Pulse Dispersion and Shaping in Microstrip Lines

JOHN F. WHITAKER, STUDENT MEMBER, IEEE, THEODORE B. NORRIS, G. MOUROU, AND THOMAS Y. HSIANG, MEMBER, IEEE

Abstract—**A method for determining the modal dispersion of gigahertz-bandwidth pulses on microstrip transmission lines is described. We have investigated the evolution of temporal waveforms propagating on microstrips, with very good agreement noted between experimental pulse shapes and numerical simulations. The resulting pulse distortion contributed to a pulse-shaping application where 100-ps rise times were stretched to the nanosecond durations necessary to control the shape of high-energy optical pulses used in fusion research. The tunability of the shape of the rising edge was investigated through variation of the stripline geometry and the substrate material. Additional effects due to high-frequency attenuation in several dipolar liquid dielectrics were substantiated experimentally, and the relevance of the results has been discussed.**

I. Introduction

As THE SIZE of electrical devices decreases and the bandwidth they are expected to respond to increases, the study of the propagation of ultrafast transients becomes important. The operation of practical devices in the millimeter-wave range has already been demonstrated [1], and the generation of electrical signals with terahertz components has also been accomplished [2]. The problems associated with the creation, detection, and characterization of these signals have been in large part solved [3], [4], leaving the study of transmission until last [5], [6]. This paper considers the propagation of signals that contain high-frequency spectral components in microstrip transmission lines, as well as applications to controlled pulse shaping.

The microstrip is intrinsically dispersive—it is incapable of supporting a pure TEM wave [7]. The inhomogeneous dielectric experienced by the fringing field of the microstrip leads to a discontinuity of the field at the interface (Fig. 1) and, ultimately, the presence of contributions from longitudinal components. To describe the permittivity encountered by a wave on a guiding structure that contains the air–dielectric interface, the concept of an effective dielectric constant is introduced [8]. This is a quantity which is always smaller than the permittivity of the substrate, since the fringing field exists partially in air and not exclusively in the substrate. It describes the interaction of the field with a dielectric which is both the substrate and the open air. Also, owing to the non-TEM nature of this transmission line, it is dependent on the frequency of a signal. Qualitatively, more of the field lines are in the dielectric at high frequencies than at low frequencies, leading to an effective permittivity that increases with frequency.

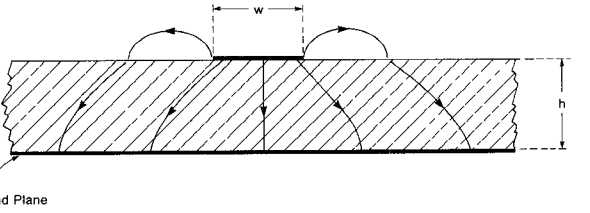

Fig. 1. Transverse cross section of microstrip with discontinuous electric-field lines shown.

The low-frequency regime can be described by a quasi-static analysis [9], [10], where results have indicated dispersionless operation. The TEM mode propagation has been assumed in fashioning design equations:

$$\epsilon_{\text{eff}} = \frac{1}{2}\left\{(\epsilon_r+1)+(\epsilon_r-1)(1+10h/w)^{-1/2}\right\} \quad (1)$$

where h is the spacing of the microstrip electrodes, w the width of the top electrode, and ϵ_r the relative permittivity of the substrate. Full-wave analyses [11], [12] and semiempirical techniques [13], [14] to generate closed-form expressions for the frequency-dependent dielectric function have also been developed, providing more realistic information as higher frequencies and modes become present. When a curve is fit from this analysis [15], the effective permittivity is found to behave as shown in Fig. 2, calculated for a microstrip containing water as a substrate with $h = w = 1$ cm. This curve has the form

$$\sqrt{\epsilon_{\text{eff}}(f)} = \sqrt{\epsilon_{\text{eff}}} + \left(\sqrt{\epsilon_r} - \sqrt{\epsilon_{\text{eff}}}\right) \Big/ \left(1+4F^{-3/2}\right) \quad (2)$$

where

$$F = (f/c)\left(4h\sqrt{\epsilon_r - 1}\right)\left\{1/2+(1+2\log(1+w/h))^2\right\} \quad (3)$$

and c is the speed of electromagnetic radiation in vacuum. A significant change in the effective permittivity is observed, taking place over several decades of frequency. If a

Manuscript received February 24, 1985; revised July 19, 1986. This work was supported in part by the U.S. Department of Energy Office of Inertial Fusion under agreement No. DE-FC08-85DP40200, the sponsors of the Laser Fusion Feasibility Project at the Laboratory for Laser Energetics, and the National Science Foundation under Grant ECS-8306607.

J. F. Whitaker, T. B. Norris, and G. A. Mourou are with the Laboratory for Laser Energetics, University of Rochester, Rochester, NY 14623–1299.

T. Y. Hsiang is with the Department of Electrical Engineering, University of Rochester, Rochester, NY 14627.

IEEE Log Number 8611015.

0018-9480/87/0100-0041$01.00 ©1987 IEEE

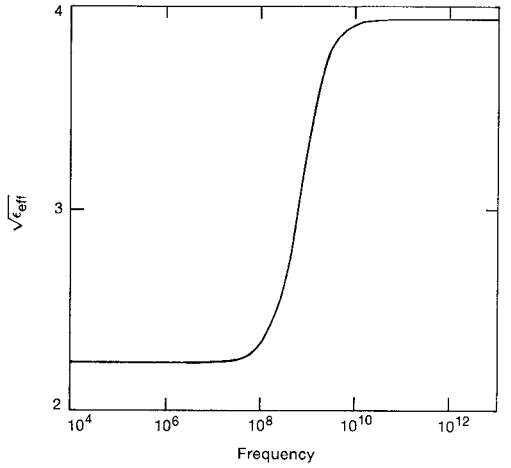

Fig. 2. The frequency dependent effective dielectric function for a microstrip of $w = h = 1$ cm and $\epsilon = 80$ (water).

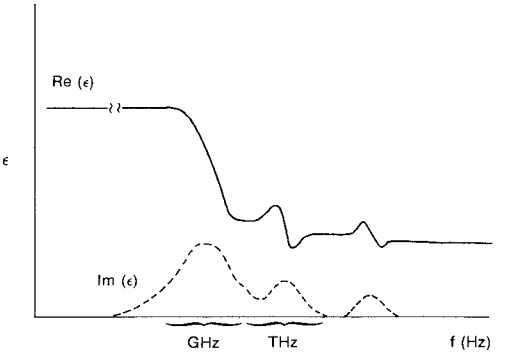

Fig. 3. The real and imaginary parts of the relative permittivity of a hypothetical material showing a dipolar relaxation, an ionic resonance, and an electronic resonance (left to right) (from [17]).

pulse contains frequency components in the region where ϵ_{eff} varies significantly, dramatic changes in the shape of a waveform will result from the action of this function.

The propagation velocity of a signal depends on the effective permittivity as $v = c/\sqrt{\epsilon_{eff}(f)}$, so that the signal velocity varies with frequency inversely to the behavior shown in Fig. 2. As a consequence, spectral components below the transition in Fig. 2 propagate with one velocity, while the higher frequencies travel at another, lower velocity. This modal dispersion leads to distortion of the temporal waveform as it propagates on the microstrip. The dispersion, however, is not present due to the onset of attenuation, as might be expected considering the coupling between loss and dispersion via the Kramers–Křonig relations [16]. These expressions relate the real and imaginary parts of the permittivity of a material, and require that dispersion of a signal in a material be impossible without attenuation, and vice versa. In the case of the effective permittivity, though, the geometry of the microstrip does not lead to coupling between the real and imaginary parts. This is because the geometry-dependent dispersion takes place as a result of redistribution of energy from the TEM mode to higher order modes (such as TE), not because of any connection with attenuation. The transition from lower to higher dielectric constant occurs in the region of frequencies where the wavelength in the dielectric is on the order of the transverse dimensions of the microstrip. While it is true that the skin effect attenuation is dependent on the geometry of the microstrip, it is not connected to the modal dispersion in the manner that dielectric absorption is related to material-dependent dispersion, as in a dipolar relaxation or an ionic or electronic resonance. An example of the real and imaginary parts of the dielectric function for a hypothetical material displaying all three is given in Fig. 3 [17]. These material effects will constitute the basis for a future paper, although their consequences will be discussed briefly later in this paper where it is believed they have influenced, in some instances, the propagation of waveforms in the presence of modal dispersion.

A useful reference quantity which identifies the approximate center of the transition of the effective permittivity function is the cutoff frequency

$$f_{TE} = c/4h\sqrt{\epsilon_r - 1}\,. \tag{4}$$

From this expression one can determine the region where the first longitudinal mode—TE for microstrip—contributes significantly. In general, a microstrip can be expected to preserve the rise time of a temporal pulse if the rising edge contains only spectral components at frequencies less than one decade below the cutoff (Fig. 2). If a signal possesses a bandwidth reaching above this point, it will be distorted with propagation distance until eventually the spectrum of the rise time contains only frequencies below cutoff. Therefore, in order to keep the effect of modal dispersion low, the cutoff frequency should be kept high. This indicates that the impediments to ultrafast propagation on microstrip, at least to first order, are large electrode spacings and high relative dielectric constants.

Though the effects of dispersion can be detrimental, as for example by imposing speed limitations on digital circuits, they can also be exploited for another practical application. This involves employing dispersion as the basis for a flexible waveform-shaping system. Laser-driven inertial fusion targets require carefully controlled temporal shaping of the optical driver pulse to achieve high performance. In fusion applications, an optical pulse propagates through many stages of amplification and experiences a great deal of gain. This amplification is not uniform, and the temporal gain profile indicates that saturation occurs early in the duration of a waveform, resulting in pulse distortion. By properly shaping the input laser pulse, however, it is possible to compensate for the effects of the amplifiers. For example, it has been calculated at the Lawrence Livermore National Laboratory that an input of the shape shown in Fig. 4 is needed for the Nova laser system to attain a square output optical pulse [18], the waveform most efficiently absorbed by a target. The shaping of the input optical pulse involves the application of specific electrical waveforms to an electrooptic crystal. Synchronized to this transient in the crystal is a low-energy, square, optical input pulse, which can thus take on the shape of the electrical waveform. The concept of a

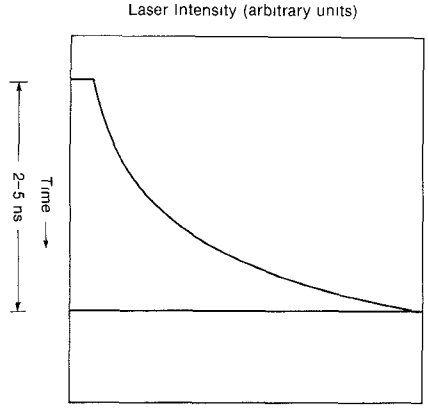

Fig. 4. The required input optical pulse shape to compensate for amplifier saturation in the Nova laser system. To attain a square output waveform, a rise time duration of 5 ns may be needed. The progression of time is indicated by the arrow; the same convention will be used in all subsequent figures.

dispersive transmission line can be extended to that of a pulse-shaping system, which uses dispersion to generate waveforms that have amplitudes increasing monotonically in time on the nanosecond or subnanosecond timescale required for laser fusion. By simply propagating a signal on the correct dispersive line, a properly shaped waveform will appear at the output.

To date, these shaped electrical transients have been generated using frozen wave generators [19]–[21] and a tapered-line pulse shaper [22]. These methods rely on continuous impedance mismatches or on the activation of many photoconductive elements, and they appear to be more complicated than a method employing the dispersive properties of a transmission line near its cutoff frequency. The shape of a pulse can be tuned by adjusting the parameters of the microstrip: cross-sectional geometry, length of propagation, and dielectric material. Through variation of these, different cutoff frequencies have been selected and their effects observed.

In this paper, computational and experimental results on the characteristics of pulse dispersion and the technique of pulse shaping in microstriplines are reported. Section II describes a practical algorithm that uses dispersive properties of microstrip at single frequencies to analyze the evolution of guided transients. Experimental verifications of the computed predictions are presented in Section III, and the initial results indicating the utility of dispersion in pulse shaping are discussed in Section IV. Section V summarizes the work and projects the investigations to be undertaken in the next phase.

II. Computation

In order to illustrate the effects of dispersion on a pulse, calculations of the propagation of waveforms in microstrip have been carried out. Using the expression for permittivity given earlier, a computer algorithm was generated to simulate the evolution of a pulse on a microstrip with any dimensions. An input, $v(\tau,0)$, with either Gaussian or exponential characteristics, or digitized from experimental information, was transformed via discrete Fourier techniques to yield the input spectrum: $F\{v(\tau,0)\}$. It is this quantity which was acted upon by the frequency-dependent characteristics of the line

$$F\{v(\tau,0)\}\cdot\exp(-\gamma(f)z) \tag{5}$$

where $\gamma(f)$ was the propagation factor for microstrip, and z the propagation distance. The distorted temporal pulse was returned after an inverse Fourier transform

$$v(\tau,z)=F^{-1}\{F\{v(\tau,0)\}\cdot\exp(-\gamma(f)z)\}. \tag{6}$$

The propagation factor consisted of two parts: a phase factor $\beta(f)$ and an attenuation function $\alpha(f)$

$$\gamma(f)=\alpha(f)+j\beta(f). \tag{7}$$

For the case of a nonmagnetic, lossless substrate, the phase factor was given by

$$\beta_0(f)=(2\pi f/c)\sqrt{\epsilon_{\text{eff}}(f)}. \tag{8}$$

The attenuation factor was actually divided into two parts, that due to the conductive electrodes and that due to shunt conductance through the dielectric. The skin effect was given by the abbreviated expression [23]

$$\alpha_c=\left(0.072\sqrt{f}\lambda_g\right)/wZ_0 \tag{9}$$

in dB/microstrip wavelength. Here, f was in gigahertz, Z_0 was the characteristic impedence, and λ_g the microstrip wavelength

$$\lambda_g=\lambda_0/\sqrt{\epsilon_{\text{eff}}(f)} \tag{10}$$

where λ_0 is the free-space wavelength. It was also necessary to recall that Z_0 is dependent on $\epsilon_{\text{eff}}(f)$, and thus also on frequency [9]

$$Z_0=\eta_0/\left(\sqrt{\epsilon_{\text{eff}}(f)}\,\text{F}(w/h)\right) \tag{11}$$

where

$$\text{F}(w/h)=2\pi(\ln(8h/w)+0.25(w/h))^{-1} \quad \text{for } w/h<1 \tag{12a}$$

or

$$\text{F}(w/h)=w/h+1.393+0.667\ln(w/h+1.444) \quad \text{for } w/h>1 \tag{12b}$$

and where η_0 was the impedance of free space, 377 Ω. The dielectric loss was given by [23]

$$\alpha_d=27.3\epsilon_r(\epsilon_{\text{eff}}(f)-1)(\tan\delta)/\{\epsilon_{\text{eff}}(f)(\epsilon_r-1)\} \tag{13}$$

in dB/microstrip wavelength, where $\tan\delta$ is the loss tangent, $\text{Im}(\epsilon_r)/\text{Re}(\epsilon_r)$, a characteristic of the substrate.

Except in the case of a material relaxation or resonance, when the loss tangent increases and losses become high, the dielectric loss will be nearly negligible (less than 0.05 dB/mm for $\epsilon_r=10$ at 10 GHz). This was assumed to be true in our calculations. In a similar situation, the conductor losses were found to be moderate (less than 0.25 dB/mm), but significant enough to be included in the algorithm. Finally, the full phase factor for an arbitrary transmission line with negligible shunt conductance was

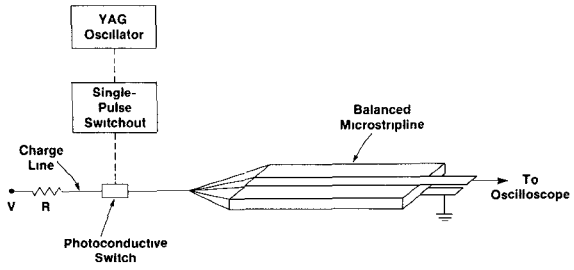

Fig. 5. A schematic for a system using laser-driven pulse excitation of a microstrip to study waveform dispersion.

given by

$$\beta(f) = \sqrt{\beta_0^2(f) + \alpha^2(f)}\,. \tag{14}$$

This expression for phase, along with the skin-effect loss, was used to calculate the propagation factor and the dispersion at any place on an arbitrary microstrip. This capability allowed us to predict the outputs of specific lines without having to build them. It thus saved much time from the process of selecting substrate materials and stripline geometries which would provide interesting results.

III. Experimental

The schematic of a system used to observe the effects of modal dispersion on a fast waveform is shown in Fig. 5. A section of RG-58 coaxial cable was used as a charge line with a system consisting of a single microstrip transmission line with its top electrode interrupted by a 500-μm-long piece of CdSe semiconductor. The cable with a 20-kΩ charging resistor, biased at 200 V dc, stores charge due to the high resistivity of the CdSe element. This switch was activated by a single 100-ps FWHM excitation pulse with a wavelength of 1.06 μm, electrooptically selected from a CW mode-locked, Q-switched Nd:YAG laser. A pulse energy of 60 μJ, focused onto the CdSe with both spherical and cylindrical lenses, was needed to close the switch and attain a switching efficiency of 10 to 20 percent, a low value due to the poor absorption of this infrared wavelength by CdSe. The optical pulse energy was integrated by the photoconductor—barring saturation by the switch—so that the electrical waveform exhibited a rise time of about 100 ps, while the pulse duration was determined by the natural recombination of the semiconductor or the length of the charge line, whichever was shorter. The resulting output was a baseband signal containing frequency components up to 3.5 GHz.

The electrical signal was coupled to the dispersive microstrip via a Tektronix 18-GHz flexible coaxial cable with SMA connectors. The microstrip was restricted in the sense that the line was to have a cutoff value which significantly affected a wide range of frequencies up to 3.5 GHz. In addition, it was necessary for the line to have low shunt loss and impedance matching capability. In order to attain the necessary cutoff criterion, a thick (2.54 cm) slab of acrylic ($\epsilon_{dc} = 2.46$) was inserted as the substrate. Copper foil electrodes of equal size (5 cm wide) supported the electrical signal in a balanced microstrip geometry—fundamentally the same as a pure microstrip configuration with h replaced by $h/2$ in the design equations. This actually led to the erroneous production of a line with a characteristic impedance of 27.5 Ω, although the resulting mismatch with 50-Ω cable was corrected by tapering the height and width of the microstrip at its input. The shunt conductance of the acrylic was known to be low, since there were no significant resonances or relaxations below 3.5 GHz.

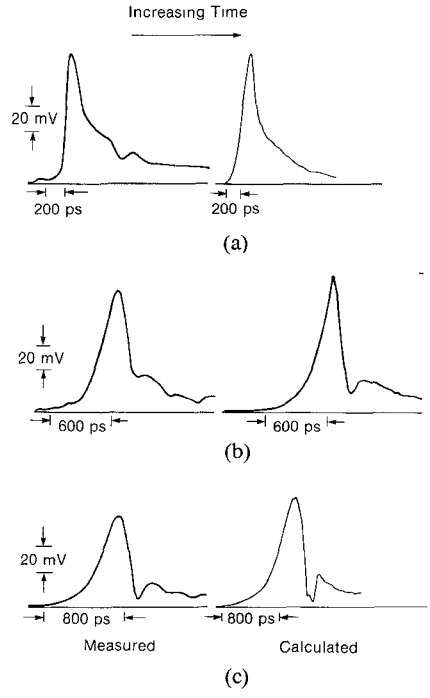

Fig. 6. The comparison of experiment (left) and computation of the evolution of a 100-ps rise time pulse as it propagates on a microstrip with an acrylic substrate: (a) input, (b) 82.1 cm, (c) 137.7 cm. The ordinate in all figures is voltage, and for the computed results, the voltage scale is arbitrary.

The cutoff, calculated to be about 4.8 GHz, was chosen so that frequencies down to less than 500 MHz would be affected by the onset of modal dispersion. In addition, the microstrip was cut into several segments, each of different length, so that the dispersion could be observed as a function of the length of propagation along the line. The progress of an experimentally dispersed pulse is demonstrated in Fig. 6, along with the computed results. The input pulse (a), as well as waveforms detected after 82.1 cm (b) and 137.7 cm (c) of propagation, is presented. Each of the experimental pulses was detected and displayed using a Tektronix S-6 sampling head in a 7834 storage oscilloscope.

The input to the dispersive line, the same as the switch output, was a waveform consisting of a 100-ps rise time, limited by the excitation pulse, and a 10–15-ns decay duration, due to the relaxation mechanisms in the CdSe switch. The digitized pulse for the algorithm was 512 points long and did not include the disturbance on the real trailing edge which resulted from a reflection. The dis-

torted waveforms exhibited rising edges which were much longer than that of their input. The fast, 100-ps components occurred later in the pulse, indicating that they were delayed with respect to the slower components. In other words, the transient appeared to be nearly reversed in time, with the lower frequency components appearing first, and the higher ones last. The trend continued with propagation distance, as can be seen in Fig. 6 (b), where the rise time was found to be 320 ps, and in Fig. 6 (c), where it was 400 ps. From the waveform calculations, these values were determined to be 350 ps and 415 ps, respectively. Additionally, the position and 100-ps duration of the fast components of the pulse were faithfully reproduced. Thus, a quantitative agreement, even with many of the fine features represented by the computation, was obtained between the experimental and computed results.

An interesting feature of the calculated waveforms in Fig. 6 is that the peak value of the pulse, as shown in (b), appears to have a larger magnitude than that in (a). This occurs as a result of the temporary pulse compression, when the components at low frequencies "catch up" with those at higher frequencies. This effect quickly diminishes as the pulse propagates further, as shown in Fig. 6(c). Similar effects have been observed by Li *et al.* [24]. It should also be noted that the transient analysis of Djordjevíc *et al.* [25] does not indicate any pulse sharpening on an arbitrary multiconductor transmission line. This calculation was, however, a distributed-circuit analysis, and it does not represent the unique geometrical factors of the microstrip affecting the quasi-TEM mode of propagation. It is, therefore, not entirely clear why the enhanced peak is not observable in our experimental results, although it may be true that the signals have simply been diminished by leakage [26] unaccounted for in our algorithm.

IV. Pulse Shaping

From parts (b) and (c) of Fig. 6, it is seen that the general waveform shape needed for fusion applications, as shown in Fig. 4, can be produced through the dispersion of an electrical pulse on microstrip. As indicated earlier, the pulse shape can be tuned via adjustment of the microstrip parameters until the specified shape is attained. Since the shapes generated for arbitrary line parameters can be reliably calculated, as has been demonstrated, it was only necessary to determine the values for the material permittivity and the geometry of the line which would yield the desired computed shape. A microstrip with the calculated parameters was then built to generate a wave shape as computed.

To realize such a pulse-shaping scheme, it was first necessary to note that the cutoff frequency must be kept low in order for a microstrip to affect the 3.5-GHz bandwidth pulse, and that to honor (4) the substrate height and dielectric constant values must therefore be great. For example, in one case it was discovered that a cutoff on the order of several hundred megahertz was desirable, and to keep the height manageable ($h \leqslant 5$ cm), a permittivity of

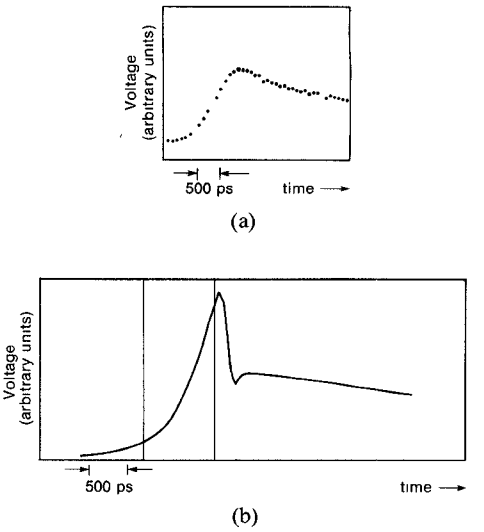

Fig. 7. The experimental (a) and computed (b) response of 25 cm of microstrip to a 100-ps input (methanol substrate). The section indicated in (b) is the part of the pulse used in the pulse-shaping application.

10 to 100 was needed. Some of the readily available materials satisfying this requirement included zirconium silicate ($\epsilon_{dc} \simeq 10$), a mixture of titanium dioxide crystals milled from rutile ($\epsilon_{dc} = 114$) [27], and a collection of polar liquids: acetone ($\epsilon_{dc} = 20.7$), ethanol ($\epsilon_{dc} = 24.3$), methanol ($\epsilon_{dc} = 32.6$), and distilled water ($\epsilon_{dc} = 80.1$) [28]. The choice of substrate material immediately fixed one parameter, leaving the dielectric height, electrode width, and propagation distance to be varied. The electrode width, affecting the dispersion the least, was changed only in conjunction with h in order to maintain an impedance of about 50 Ω. Thus, for any one material, the height (already constrained to a maximum value) and length of a microstrip would be modified until an acceptable waveform was computed.

The various microstrips were constructed, with the zirconium silicate powder contained in a box with plexiglass sides and a 0.32-cm-thick copper ground plane on the bottom. A thin sheet of plastic covered the top, and the packed powder itself supported the copper electrode, tapered at the ends for coupling purposes. The liquids were enclosed in plastic bags with negligibly thin walls, and these in turn were placed on a copper ground plane between two aluminum mounts, supporting the SMA-to-microstrip launchers which were connected with the top electrode. This copper foil strip was tapered in width at its ends and also conformed with the taper of the bag near the connectors. Liquid could be conveniently added or removed from the bags to change the height and dispersion of a line.

Fig. 7(a) shows the experimental dispersed output for a 25-cm section of microstrip containing a dielectric of ethanol 2 cm thick. This can be compared with Fig. 7(b), the expected result via calculation, to see that the values of the rise times agree to within several percent. Additionally, the experimental curves for the following microstrips are displayed in Fig. 8: (a) 25-cm-long, 2-cm-thick methanol substrate; (b) 150-cm-long, 5-cm-thick zirconium silicate

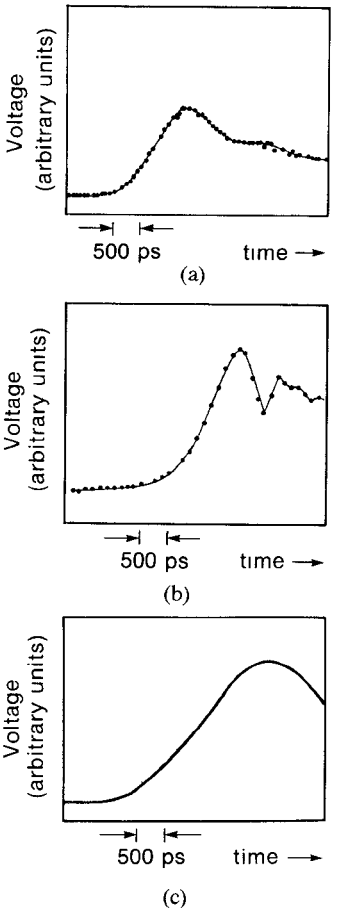

Fig. 8. Experimental pulse shapes from microstrips containing (a) methanol, (b) zirconium silicate, and (c) distilled water. The points in (b) and (c) are the actual trace from the sampling oscilloscope; the line through them is to clarify their path.

substrate; and (c) 25-cm-long, 2-cm-thick distilled water dielectric. For each of these lines, a 100-ps rise time was stretched to a duration of several nanoseconds. The water-line, which had the highest permittivity of any of the structures, provided the greatest rise time, 2.5 ns. This rising edge was longer than that produced from even the much thicker, much longer zircon-line, having a permittivity eight times lower. This indicated that a relatively compact unit could be fabricated with water for the purpose of generating long, tunable, electrical waveforms.

Furthermore, it was noted that delayed fast components predicted by the computation of dispersion on the ethanol-line were not present experimentally (Fig. 7(a)). In fact, the high-frequency components were noticeably lacking from the dispersed waveforms for all the lines containing polar liquids. It was thus discovered that the dipolar nonresonant absorption indicated hypothetically in Fig. 3 affected the propagation of these 3.5-GHz bandwidth pulses [29]. Both anomalous dispersion and attenuation would take place if the real and imaginary parts of the permittivity influenced the signal. However, the attenuation over the long propagation distances involved has evidently negated the dispersion and simply left the transient without its original high-frequency characteristics, acting somewhat as a low-pass filter [30], [31].

V. Summary

Microstrip transmission lines have been used to study modal dispersion and its application to electrical and optical pulse shaping for use in fusion energy research. We have also verified the accuracy of a method which computes the shape of fast waveforms propagating on arbitrary microstrips. Although the discussion has been limited to pulses with bandwidths in the low microwave regime, material effects have been substantiated and the stage is set for further work in microwave spectroscopy using dispersion in transmission lines.

To determine the properties of materials by utilizing them as substrates in transmission lines, it will first be necessary to increase the frequencies present by decreasing the duration of the pulse rise times. In addition, a system will be needed for characterizing these ultrafast signals. These tasks shall be accomplished through use of an electrooptic sampling system driven by a colliding-pulse, mode-locked dye laser [1]–[4]. This system produces optical pulses with duration of about 100 fs, and is thus capable of exciting transmission lines to frequencies in the far-infrared region of the spectrum. The shortest event realized thus far possessed a duration of less than half a picosecond, leading to speculation that millimeter or submillimeter spectroscopy may be possible.

References

[1] K. E. Meyer, D. R. Dykaar, G. A. Mourou, and T. Y. Hsiang, "Characterization of TEGFET's and MESFET's using the electro-optic sampling technique," presented at the 1985 OSA Topical Meeting on Picosecond Electronics and Optoelectronics, Incline Village, NV, March 14, 1985; to be published in the conference proceedings.

[2] G. A. Mourou and K. E. Meyer, "Subpicosecond electrooptic sampling using coplanar strip transmission lines," *Appl. Phys. Lett.*, vol. 45, no. 5, pp. 492–494, Sept. 1, 1984.

[3] J. A. Valdmanis, G. A. Mourou, and C. W. Gabel, "Picosecond electrooptic sampling system," *Appl. Phys. Lett.*, vol. 41, no. 3, pp. 211–212, Aug. 1, 1982.

[4] J. A. Valdmanis, G. A. Mourou, and C. W. Gabel, "Subpicosecond electrical sampling," *IEEE J. Quantum Electron.*, vol. QE-19, pp. 664–667, Apr. 1983.

[5] G. Hasnain, G. Arjavalingam, A. Dienes, and J. R. Whinnery, "Dispersion of picosecond pulses on microstrip transmission lines," in *Proc. SPIE Conf.* (San Diego), 1983.

[6] C. J. Kryzak, S. M. Faris, K. E. Meyer, and G. A. Mourou, "Transmission line designs with a measured step response of 3 ps/cm," presented at the 1985 OSA Topical Meeting on Picosecond Electronics and Optoelectronics, Incline Village, NV, March 14, 1985; to be published in the conference proceedings.

[7] T. C. Edwards, *Foundations for Microstrip Circuit Design*. Chichester: Wiley, 1981.

[8] For example, see K. C. Gupta, R. Garg and I. J. Bahl, *Microstrip Lines and Slotlines*. Dedham, MA: Artech House, 1979, ch. 1.

[9] H. A. Wheeler, "Transmission line properties of parallel strips separated by a dielectric sheet," *IEEE Trans. Microwave Theory Tech.*, vol. MTT-13, pp. 172–185, 1965.

[10] M. V. Schneider, "Microstrip lines for microwave integrated circuits," *Bell Syst. Tech. J.*, vol. 48, pp. 1422–1444, 1969.

[11] R. Mittra and T. Itoh, "A new technique for the analysis of the dispersion characteristics of microstrip lines," *IEEE Trans. Microwave Theory Tech.*, vol. MTT-19, pp. 47–56, 1971.

[12] T. Itoh and R. Mittra, "Spectral-domain approach for calculating dispersion characteristics of microstrip lines," *IEEE Trans. Microwave Theory Tech.*, vol. MTT-21, pp. 496–498, 1973.

[13] W. J. Getsinger, "Microstrip dispersion model," *IEEE Trans. Microwave Theory Tech.*, vol. MTT-21, pp. 34–39, Jan. 1973.

[14] G. Kompa and R. Mehran, "Planar waveguide model for calculating microstrip components," *Electron. Lett.*, vol. 11, pp. 459–460, 1975.
[15] E. Yamashita, K. Atsuki, and T. Ueda, "An approximate dispersion formula of microstrip lines for computer-aided design of microwave integrated circuits," *IEEE Trans. Microwave Theory Tech.*, vol. MTT-27, pp. 1036–1038, 1979.
[16] J. D. Jackson, *Classical Electrodynamics*. New York: Wiley, 1975, pp. 284–326.
[17] C. Kittel, *Introduction to Solid State Physics*, 5th ed. New York: Wiley, 1976, ch. 13.
[18] L. M. Franz and J. S. Nodvik, "Theory of pulse propagation in a laser amplifier," *J. Appl. Phys.*, vol. 34, no. 8, 1963, pp. 2346–2349.
[19] J. M. Proud, Jr. and S. L. Norman, "High-frequency waveform generation using optoelectronic switching in silicon," *IEEE Trans. Microwave Theory Tech.*, vol. MTT-26, pp. 137–140, 1978.
[20] C. S. Chang, M. C. Jeng, M. J. Rhee, Chi H. Lee, A. Rosen, and H. Davis, "Direct dc to rf conversion by picosecond optoelectronic switching," in *1984 IEEE MTT-S Int. Microwave Symp. Dig.*, pp. 540–541.
[21] J. F. Whitaker, D. Smith, and G. A. Mourou, "Electronic pulse shaping using multiple solid-state switches," presented at the 1983 IEEE Conference on Electron Device Activities in Western New York, Rochester, NY, Oct. 18, 1983.
[22] G. M. McWright, "Simplified theory of variable impedance stripline under pulse excitation," to be published.
[23] E. O. Hammerstad and F. Bekkadal, "A microstrip handbook," ELAB Report, STF 44 A74169, Univ. of Trondheim, Norway, pp. 98–110, 1975.
[24] K. K. Li, G. Arjavalingam, A. Dienes, and J. R. Whinnery, "Propagation of picosecond pulses on microwave striplines," *IEEE Trans. Microwave Theory Tech.*, vol. MTT-30, pp. 1270–1273, 1982.
[25] A. R. Djordjevíc, T. K. Sarkar, and R. F. Harrington, "Analysis of lossy transmission lines with arbitrary nonlinear terminal networks," *IEEE Trans. Microwave Theory Tech.*, vol. MTT-34, pp. 660–666, 1986.
[26] A. A. Oliner and K. S. Lee, "The nature of the leakage from higher order modes on microstrip line," in *1986 IEEE MTT-S Int. Microwave Symp. Dig.*, pp. 57–60.
[27] J. D. Kraus and K. R. Carver, *Electromagnetics*. New York: McGraw-Hill, 1973, p. 58.
[28] *Handbook of Chemistry and Physics*, R. C. Weast, Ed. Cleveland, OH: Chemical Rubber Company Press, 1973, section E, pp. 55–60.
[29] J. B. Bicks and J. Hart, Eds., *Progress in Dielectrics*, vol. 4. New York: Academic Press, 1962, pp. 39–94.
[30] N. S. Nahman, R. M. Jickling, and D. R. Holt, "Reference-waveform generation using Debye dielectric dispersion," *Nat. Bur. Stand. (U.S.) NBSIR 73-304*, Dec. 1972.
[31] J. Andrews, "Pulse reference waveform standards development at NBS," in *Proc. Automated Testing for Electronics Manufacturing Seminar/Exhibit*, Jan. 1981, pp. IV-3–IV-19.

✠

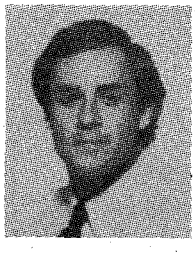

John F. Whitaker (S'84) was born in Penn Yan, NY, on March 3, 1959. He received the B.S. degree in physics from Bucknell University, Lewisburg, PA, in 1981, and the M.S. degree in electrical engineering from the University of Rochester, Rochester, NY, in 1983.

He is currently a doctoral candidate in electrical engineering, studying optical electronics in the Ultrafast Science Division at the Laboratory for Laser Energetics of the University of Rochester.

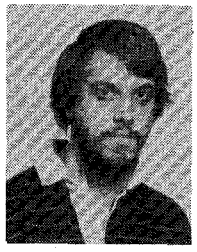

Theodore B. Norris was born in Huntingdon, PA, on December 30, 1960. He received the B.A. degree with highest honors in physics from Oberlin College, Oberlin, OH, in 1982, and the M.A. degree in physics from the University of Rochester, Rochester, NY, in 1984. He is working toward the Ph.D. degree with concentrations in optical simulation propagation and ultrashort-laser techniques.

Mr. Norris is a member of the American Physical Society, Phi Beta Kappa, and Sigma Xi.

✠

G. Mourou was born in Albertville, France, in 1944. He received the B.S. degree from the University of Grenoble, Grenoble, France, in 1967, the Doctorat de 3ème Cycle from the University of Orsay, Orsay, France, in 1970, and the Doctorate d'Etat from the University of Paris in 1973.

From 1967 to 1970, he worked at the École Polytechnique, Paris, where he studied the spectral property of the Q-switched ruby laser. From 1970 to 1979, he was at the Université Laval, Quebec, Canada, where his interest was in the study of the picosecond kinetics of dye molecules in solutions. From 1973 to 1974, he spent a postdoctoral year at the Department of Chemistry, San Diego State University, San Diego, CA, before going back to France to join the Laboratoire d'Optique Appliquée, ENSTA-Ecole Polytechnique, as a scientist. In 1977, he joined the Laboratory for Laser Energetics, University of Rochester, Rochester NY, where he is now Director of the Ultrafast Science Division and Associate Professor at the Institute of Optics. He has performed pioneering work in the development of optoelectronic sampling techniques, light-activated solid-state switching, ultrashort-pulse laers, short-pulse electron-optical technology, and high-speed diagnostic techniques.

✠

Thomas Y. Hsiang (M'81) was born in Taiwan in 1948. He received the M.A. and Ph.D. degrees from the University of California in 1973 and 1977, respectively. He was a University of California Fellow from 1971 to 1973.

He was a Research Fellow at the Ames Laboratory from 1977 to 1979, where he worked on properties of superconducting-normal metal interface. From 1979 to 1981, he was on the faculty of the Illinois Institute of Technology, where he was a faculty Research Fellow in 1982. He joined the Department of Electrical Engineering at the University of Rochester in 1981 as an Assistant Professor and became an Associate Professor in 1983. His current research interests include noise properties of semiconductor devices, high-speed phenomena in GaAs and superconducting devices and in transmission lines, process and device modeling, and nonequilibrium superconductivity.

Dr. Hsiang is a member of the American Physical Society.